Real-Time Harmonic Reduction using Synchronous PWM Control for Wound-Rotor Induction Motor

M. E. Abdel- Karim
Electrical Power and Machines Dept., Faculty of Eng.
Tanta University, EGYPT

Abstract In this paper the dynamic performance of the wound rotor induction motor operating with synchronized modulator is considered and analyzed. The proposed modulator employs a PWM transistor-controlled capacitive network in rotor circuit with a carrier frequency proportional to the rotor voltage frequency. This modulator can reduce the harmonic current components of the motor and consequently improve the motor power factor. The reduction of these components is achieved instantaneously with no need for sensing or computing the harmonics current in motor current, thus simplifying the control system. Simulated and experimental results obtained from closed loop 0.5KVA prototype confirm the feasibility and features of the proposed system.

1. Introduction

Adjustable speed control of induction motor (IM) via static power converter is increasingly based on real time digital generation of PWM waveforms. Different strategies for optimizing PWM for voltage source inverter in the stator side of IM such as synchronous, asynchronous PWM and regular sampling have been proposed and analyzed [1-8]. However, controlling the speed of wound- rotor IM can be achieved by using external variable rotor resistance or by resonating the rotor circuit using uncontrolled reactive rotor network [9]. These systems provide high starting and braking torque, improved power factor and also reacts favorably to non-sinusoidal supply voltage. For smooth variation of motor speed, the reactive rotor networks have been controlled using thyristor switches [10-12]. Also, transistor switches strategy has been proposed using non- optimal PWM techniques [13-14]. These switches lead to significant increase of harmonic distortion in machine currents. Such high power PWM electronic switches are generally operated at low-switching frequency, owing to limitation of the semiconductor switches. This needs an optimization for the PWM switching sequences, aiming at a reduction of harmonic components of the machine currents, and a reduction in torque harmonics.

Manuscript received from Dr. M. E. Abdel-Karim
Accepted on : 26 / 3 / 2002
Engineering Research Journal Vol 25, No 2, 2002 Minufiya University, Faculty of Engineering, Shebien El-Kom, Egypt, ISSN 1110-1180

… synchronized modulator is proposed for the electronic switches of the capacitive rotor network to control the speed of the wound rotor induction motor. This synchronized modulator is extended over a full fundamental period of the rotor voltage so that the switching of the capacitive rotor network is in synchronism with the rotor voltage frequency. The resulting pulse sequence exhibits quarter wave symmetry. Synchronized pulse sequences are advantageous in that the harmonic spectrum does not contain sub-harmonic components and minimize the low order harmonic distortion on the machine currents.

2. System Description

2-1. Power circuit

The schematic for the proposed synchronous PWM control for wound rotor IM is shown in Fig 1. Three capacitors are star connected to the rotor via a three-phase power controller using four IGBT switches. T_1 and T_3 are shunt switches while T_2 and T_4 are series switches. Each transistor is fed through four fast recovery diode bridge to act as ac switch as shown in Fig 1.

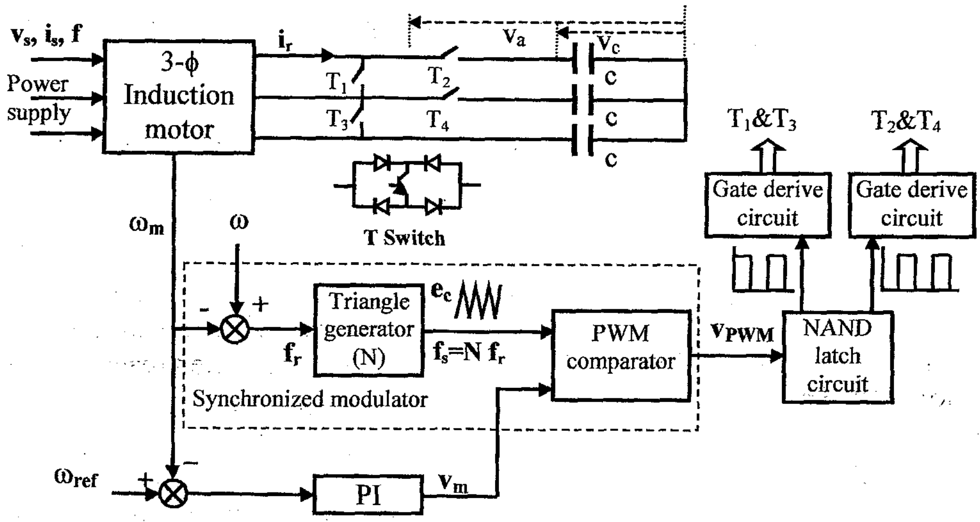

Fig. 1. Schematic diagram of the PWM with a synchronized carrier wave.

The switching process is to disconnect the capacitor (series switches are OFF while shunt switches are ON) or connect these capacitors (shunt switches are OFF while series switches are ON) in the rotor circuit. The motor rotates at its rated speed when shunt switches are continuously ON. While when the series switches are continuously ON, the capacitors are permanently connected to the rotor. To vary the motor speed over the whole range, the value of the capacitors is chosen by varying the duty cycle of the series switches from zero to 100% (i.e. from 100% to zero of the shunt switches), motor speed changes from its rated value to zero.

2-2. Control circuit

The control circuit of the system can be subdivided into synchronized modulator (for open and closed loop) and PI controller for closed loop speed regulation as shown in Fig 1. The synchronized modulator consists of a triangular carrier signal generator with output frequency f_s which is synchronized with rotor voltage frequency f_r by a fixed frequency ratio N. PWM comparator compares the synchronized-frequency carrier signal with a modulating signal v_m (open or closed loop). The comparator provides a train of synchronized pulses with a duty cycle inversely proportional to v_m and its frequency is the carrier frequency. The output of synchronized modulator is fed to the drive circuit through a NAND latch circuit. This circuit complements the synchronized pulses and ensures that, any group of series or shunt switches turned OFF just after the others are ON. The relative duty cycle of the series switches determines capacitor voltage level relative to that of the rotor and hence achieving the desired motor speed. The capacitor voltage increases due to increasing the duty cycle of series switches by reducing v_m (open loop) or ω_{ref} (closed loop).

PI controller circuit for control of a power transistor, which operate in a high frequency chopping mode, such that the duty cycle can be smoothly controlled the motor speed ω_m to the desired speed ω_{ref} in the range 0 to 100%.

3. Synchronized Modulator

Two mathematical models have been proposed for modeling the switched-control through the rotor of the induction motor [15,16]. These models are only restricted in time domain analysis. The frequency domain analysis will be used to study the motor behaviour with the proposed synchronized modulator.
In the present study, the structure considered in Fig 1, is open loop feed forward system. Effectively, the capacitors can be considered as a voltage source v_c connected to the rotor circuit and has the same rotor voltage frequency. Accordingly, the capacitor voltage v_c is sinusoidal. The switch-on duration T_{on}, Fig 2, of v_c across the rotor circuit is v_a. Due to high switching frequency, the switched voltage v_a can be approximated by a sequence of flat-topped pulses with sinusoidal shape amplitude of v_c, since the variation of $v_c(t)$ in the switching duration will not be significant. Then, $v_a(t)$ can be written as,

$$v_a(t) = \begin{cases} v_c(kT_s) & \text{for} \quad kT_s \le t < kT_s + T_{on} \\ 0 & \text{for} \quad kT_s + T_{on} \le t < (k+1)T_s \end{cases}$$

where, k = 0, 1, 2,..................

T_s is the period of switching frequency f_s.

The switched voltage $v_a^*(t)$ can be expressed as an infinite series,

$$v_a^*(t) = \sum_{k=0}^{\infty} v_c(kT_s)[u_s(t-kT_s) - u_s(t-kT_s-T_{on})] \qquad (1)$$

where $u_s(t)$ is the unit-step function.

Taking the Laplace transform, S-domain, on both sides of eq (1), it follows that,

$$V_a^*(S) = \sum_{k=0}^{\infty} v_c(kT_s)[\frac{1-e^{-ST_{on}}}{S}]e^{-kST_s} \qquad (2)$$

The term $e^{-T_{on}S}$ can be approximated by taking only the first two terms of its power-series expansion, then,

$$1-e^{-ST_{on}} = 1-[1-ST_{on} + \frac{(ST_{on})^2}{2!} - .... \cong ST_{on}$$

Thus, eq (2) is simplified to,

$$V_a^*(S) \cong T_{on} \sum_{k=0}^{\infty} v_c(kT_s)e^{-kST_s} \cong T_{on} \sum_{k=0}^{\infty} v_c(kT_s)z^{-k} \qquad (3)$$

In the Z-domain, eq (3) is equivalent to,

$$V_a(z) \cong T_{on} V_c(z) \qquad (4)$$

For the sinusoidal waveform, the Z-transform of $v_c(t)$ is [17],

$$V_c(z) = \frac{z \sin \omega_r T_s}{z^2 - 2z\cos\omega_r T_s + 1}$$

Accordingly, eq (4) becomes,

$$V_a(z) \cong T_{on} \frac{z \sin \omega_r T_s}{z^2 - 2z\cos\omega_r T_s + 1}$$

$$\cong T_{on} \frac{e^{ST_s} \sin \omega_r T_s}{e^{2ST_s} - 2e^{ST_s} \cos\omega_r T_s + 1} \qquad (5)$$

where $\omega_r = 2\pi f_r$ and f_r is the rotor voltage frequency.

For steady state $S = j\omega_r$ and $T_s = 1/f_s$ then eq (5) becomes,

$$V_a(z) \cong T_{on} \frac{e^{j2\pi\frac{f_r}{f_s}} \sin 2\pi\frac{f_r}{f_s}}{e^{j4\pi\frac{f_r}{f_s}} - 2e^{j2\pi\frac{f_r}{f_s}} \cos 2\pi\frac{f_r}{f_s} + 1} \qquad (6)$$

For fixed-frequency carrier, varying v_m will vary each of motor speed ω_m, rotor voltage frequency f_r, and switch-on duration T_{on}. Accordingly, both the phase and magnitude of $V_a(z)$ will be varied. This leads to obtaining variable harmonic current components for each motor speed.

For the proposed modulator, with a fixed frequency ratio $N = f_s/f_r$, eq (6) becomes,

$$V_a(z) \cong T_{on} \frac{e^{j2\pi/N} \sin 2\pi/N}{e^{j4\pi/N} - 2e^{j2\pi/N} \cos 2\pi/N + 1} \qquad (7)$$

The phase and magnitude of the division term in eq (7) become fixed with speed variation. However, the variation of T_{on} with motor speed will be studied as given below.

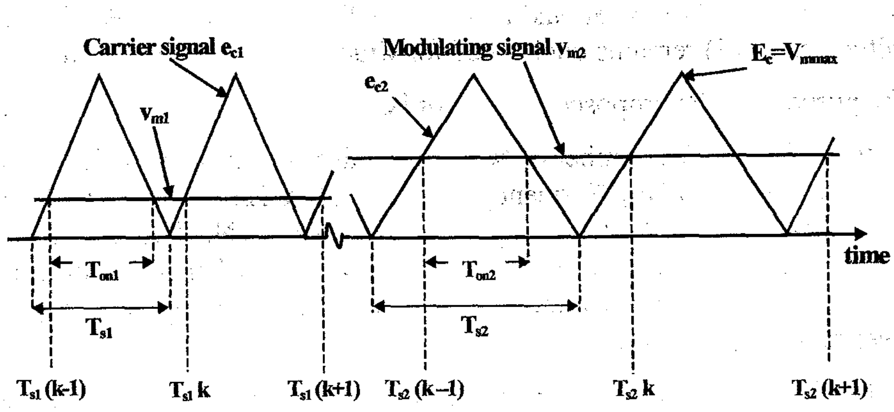

Fig. 2. Timing diagram of PWM with a synchronized-frequency carrier signal.

Figure 3, shows the speed variation versus the reference voltage v_m at certain capacitance (c=14μF) for fixed and synchronized-frequency carriers with constant load torque. Such variations was measured primarily to evaluate the behaviour of motor speed with v_m. It is noticed that the motor speed is linearly varied with v_m i.e.

$$\omega_m = k^{'}(v_m - 0.4) \tag{8}$$

Accordingly, and from Fig 2 using triangles uniformity rule,

$$\frac{T_{on1}}{T_{s1}} = f_{s1}\, T_{on1} = 1 - \frac{v_{m1}}{V_{m\,max}} \tag{9}$$

since, $\quad f_{s1} = Nf_{r1} = Ns_1 f$

$$= N\left(\frac{\omega - \omega_{m1}}{\omega}\right) f = N\left(1 - \frac{\omega_{m1}}{\omega}\right) f \tag{10}$$

where, the slip 's_1' is given by, $\quad s_1 = (\omega - \omega_{m1})/\omega$, and f is the supply frequency.

From eq (8) and by considering the synchronous motor speed $\omega = k^{'}(V_{m\,max} - 0.4)$ for simplicity, eq (10) becomes,

$$f_{s1} = \frac{N}{\xi}\left(1 - \frac{v_{m1}}{V_{m\,max}}\right) f \tag{11}$$

and eq (9) becomes,

$$\frac{N}{\xi}\left(1 - \frac{v_{m1}}{V_{m\,max}}\right) f\, T_{on1} = 1 - \frac{v_{m1}}{V_{m\,max}} \tag{12}$$

where, $\quad \xi = 1 - \dfrac{0.4}{V_{m\,max}}$

For a step change of speed reference voltage to V_{m2} at steady state, eq (12) becomes,

$$\frac{N}{\xi}\left(1 - \frac{v_{m2}}{V_{m\,max}}\right) f\, T_{on2} = 1 - \frac{v_{m2}}{V_{m\,max}} \tag{13}$$

Dividing eq (12) by eq (13) gives, $\quad T_{on1} = T_{on2} = \xi/(Nf) \quad (14)$

This means that, for the variation of speed reference voltage v_m with constant load torque, the switch-on duration T_{on} remains unchanged, while the relative duty cycle vary to ensure capacitor voltage required to achieve the desired motor speed. With this result and for constant frequency ratio N, the phase and magnitude of eq (7) remains unchanged for wide range of motor speed.

So, the purpose of the proposed modulator is,

- to maintain the number of switching pulses for the rotor voltage always fixed, i. e. the switching frequency f_s is in synchronism with the fundamental frequency of the rotor voltage f_r by the frequency ratio N. The resulting pulse sequence exhibits quarter wave symmetry such that the harmonic spectrum of the rotor voltage does not contain sub-harmonic current component, especially at lower switching frequencies.

- to change the naturally variable phase and magnitude of the switched capacitor voltage v_a, eq (6), to fixed phase and magnitude, eq (7) for wide range of motor speed. With this property of fixed phase and magnitude, the effect of the capacitor c, which can be optimally chosen at a certain speed and switching frequency to give minimum low order harmonic currents, remains valid for a wide range of motor speed.

4. Mathematical Model

Considering the per-phase equivalent circuit of the capacitor controlled IM refereed to the stator shown in Fig 4, the following motor equations can be written,

$$v_S = i_S r_S + \ell_S (di_S / dt) + i_{rm} r_m \quad (15)$$

$$i_{rm} r_m = \ell_m (di_m / dt) \quad (16)$$

$$i'_r = i_s - (\ell_m / r_m)(di_m / dt) - i_m \quad (17)$$

$$i_{rm} r_m = i'_r r'_r / s + \ell'_r (di'_r / dt) + v_a \quad (18)$$

$$v'_a = 0 \qquad \textit{if } T_a \textit{ ON and } T_b \textit{ OFF} \quad (19)$$

Hence,

$$v'_a = v'_c / s,$$

$$i'_r = s^2 c' (dv'_a / dt) \qquad \textit{if } T_a \textit{ OFF and } T_b \textit{ ON} \quad (20)$$

The developed motor torque is given by, $T_m = 3(I'^2_r\, r'_r / \omega_m)$ (21)

The electromechanical equation is given by,

$$J(d\omega_m / dt) = T_m - T_L - \beta\, \omega_m \quad (22)$$

Equations (15) to (22) have been used in ref (13) to calculate the motor performance under the condition of fixed-frequency carrier. In the present study the same equations are reprogrammed along with the following equations to simulate the system with the proposed modulator. The triangle carrier signal $e_c(t)$ of the synchronized PWM can be expressed by Fourier analysis as,

$$e_c(t) = [1 + \frac{8}{\pi^2} \sum_{n=1,3,5,...}^{\infty} \frac{1}{n^2} (-1)^{\frac{(n-1)}{2}} \sin n\omega_s t] E_c / 2 \quad (23)$$

Where E_c is the peak value of the triangular carrier signal and $\omega_s = 2\pi\, N\, s\, f$ is its angular frequency. The maximum value V_{mmax} of the modulation degree is adjusted to be equal to E_c to provide modulation degree $M = V_{mmax}/E_c = 1$.

Comparing $e_c(t)$ with $v_m(t)$ yields the switching pattern and PWM comparator V_{PWM} as,

$$V_{PWM} = V_{cc} \quad \text{for} \quad e_c(t) > v_m(t) > 0 \quad T_a \text{ OFF and } T_b \text{ ON} \tag{24}$$

$$= 0 \quad \text{for} \quad e_c(t) < v_m(t) > 0 \quad T_a \text{ ON and } T_b \text{ OFF} \tag{25}$$

Generally, with synchronized PWM modulator, $V_{PMW}(t)$ will be a periodical function with the fundamental frequency.

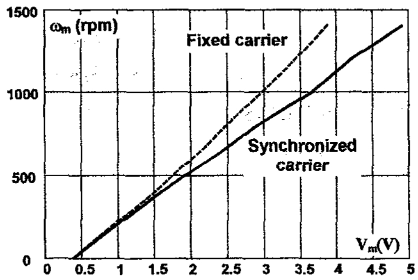

Figure 3. Measured motor speed ω_m variation with the speed reference voltage v_m.

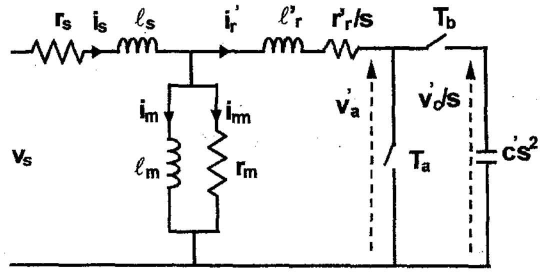

Fig. 4. Per phase motor equivalent circuit.

5. Experimental Setup

The experimental setup is illustrated in Fig 1 and was developed to test the proposed synchronized modulator for controlled wound rotor IM. The synchronized modulator is a very simple replacement of the conventional analog triangle regulator by triangular generator of FET type. The shunt (T_1 and T_3) and series (T_2 and T_4) switches are IGBT switches of type 25Q101 (V_{CEO}=1500 V, I_C=50A). An analog current controlled separately excited dc motor provides the required load torque. Parameters of employed induction and dc machines are listed in the Appendix. A PC Pentium is used to program the Lab-pc 1200 I/O card using the LabView software to display experimental data. The interface between the I/O card and the system was done via a Hall effect sensors (LA25 and LV25 from LEM) for measuring the stator and rotor phase currents and voltages, respectively. A tacho-generator with a gain 2V/1000rpm is employed for measuring the instantaneous motor speed as well as for the feedback signal. The tacho-generator output is directly connected to the I/O card. The parameters for the PC controller (kp + ki/s) were adjusted empirically by means of computer simulation for a certain operating point (at 66% of rated speed =1000r.p.m). The constant k_p for proportional controller was adjusted to 20, and the integrator k_i=80s^{-1} was used to obtain 5% overshoot of motor speed within 100 m-sec.

6. Simulation and Experimental Results

Several computer simulations and experiments were run with different operating points in order to check the performance of synchronized modulator with closed loop system. Equations (15) to (25) listed above were solved using software Matlab-Simulink to obtain the motor performance under the proposed modulator. Figures 5 and 6 show the simulated motor speed and current waveforms at the same conditions without and with the synchronized modulator, respectively. These results were taken using PI controller at different step reference voltages at 0.75 N-m load torque. The motor speeds follow the reference voltages and the steady state error for each reference is zero as shown in Figs 5a and 6a. Figure 6a ensures that the synchronized modulator makes the motor speed arrive rapidly to the reference than in Fig 5a.

Figures 5b and 6b show expanded waveforms of the applied voltage v_s, stator current i_s and referred rotor current i_r' before the sudden change of the speed reference ω_{ref} from 1200 to 800rpm. It is seen from these figures that the currents i_s and i_r' are sinusoidal due to the used synchronized modulator.

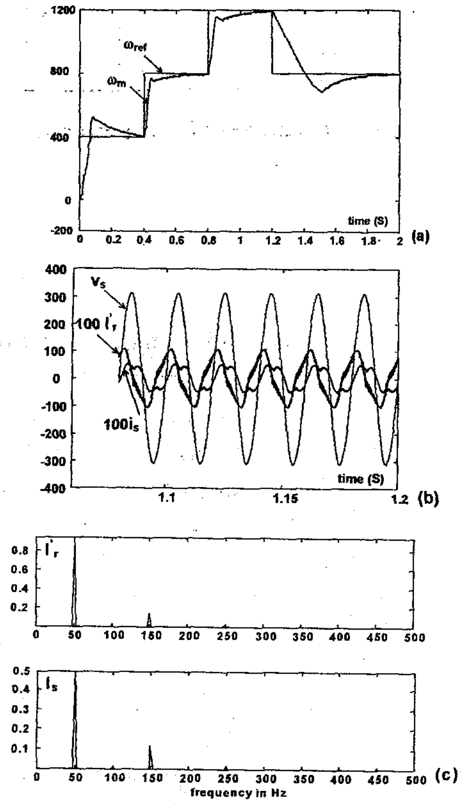

Fig. 5. Simulation results for closed loop motor control with fixed-frequency switching.

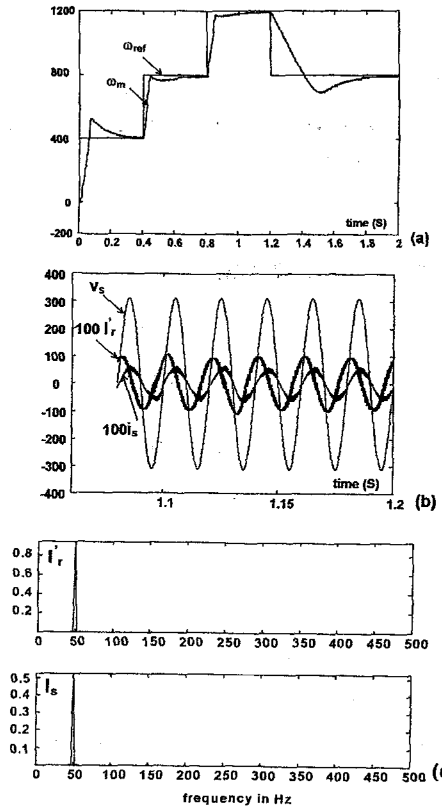

Fig. 6. Simulation results for closed loop motor control with synchronized-frequency switching.

Linear scales plot of I_r' and I_s spectra without and with the synchronized modulator are shown in Figs 5c and 6c, respectively. The results clarify the effect of the synchronized modulator in reducing the motor current harmonics produced by the fixed-frequency switching.

Figures 7 and 8 show the experimental waveforms of v_s, i_s, v_a, and i_r at closed loop motor control for a sudden change of speed reference ω_{ref} and constant load torque. In Fig 7 the speed changes from 1200 to 1040rpm with fixed switching frequency f_s is 900Hz. This low switching frequency is chosen at 1200 rpm, i.e. f_r is 10Hz, and the stator voltage v_s is reduced to 190V to have significant current harmonics and small-sustained oscillations in the motor current waveform as shown in Figs 7b and 7d. These harmonics and oscillations are increased dramatically when the speed is decreased to 1000rpm, i.e. f_r increased to 16.667Hz while the switching frequency remains without change at 900Hz.

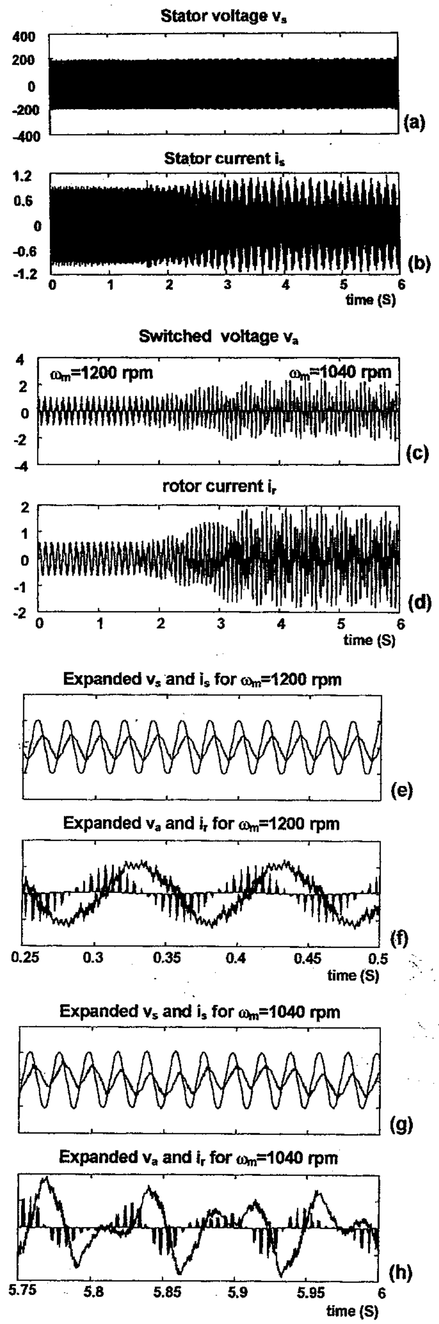

Fig. 7. Experimental results for closed loop motor control with fixed-frequency switching for speed reference variations at constant load and V_s=190V.

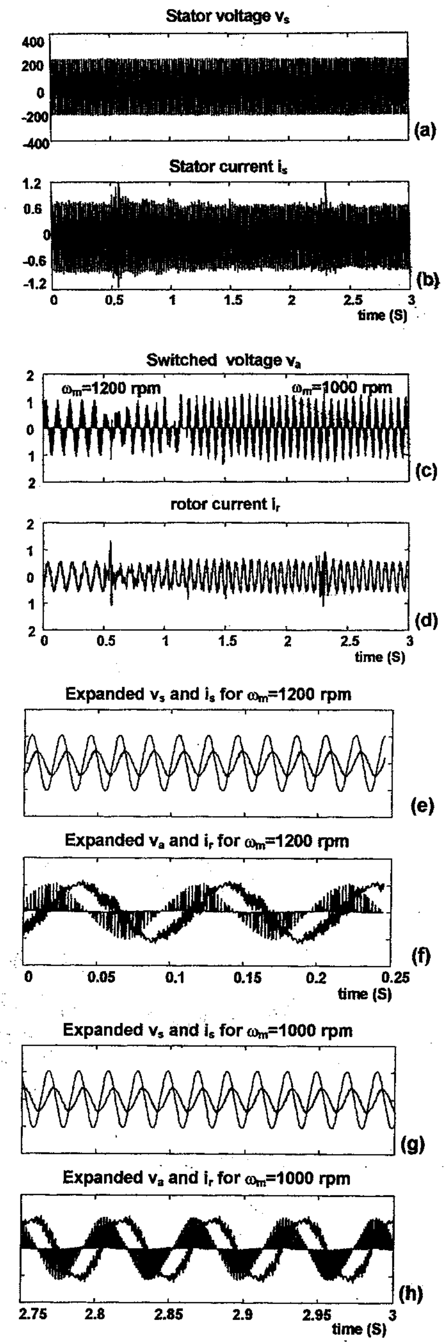

Fig. 8. Experimental results for closed loop motor control with synchronized-frequency switching for speed reference variations at constant load and V_s=220V.

In Fig 8, the synchronized modulator with fixed frequency ratio N of 90 is used. This ratio can be changed to the values with only a small adjustment in triangle generator shown in Fig 1. Figure 8 shows the system response, since the motor speed is varied from 1200 to 1000rpm with v_s 220V. Accordingly, f_r is varied from 10 to 16.667 Hz, consequently the synchronized modulator adapt f_s from 900 to 1500Hz respectively. As expected from the analysis of the proposed modulator and referring to eq (7), where the phase and magnitude of v_a remains unchanged, the motor current waveforms remain sinusoidal in the steady state for both speeds of 1200 and 1000rpm. This is true except with high switching ripple super-imposed on the motor currents

Figure 9 shows the experimental waveforms of i_{Lref}, ω_m, v_a, and i_r for closed loop motor control with synchronized switching frequency with step change of load torque at constant reference speed. Figures 9e to 9h show that, the steady state motor currents remain nearly sinusoidal before and after loading. These results according to eq (7) where only the phase of v_a remains unchanged while its magnitude is continuous variation due to the dependency of T_{on} on load value. This leads to the nearly sinusoidal appearance.

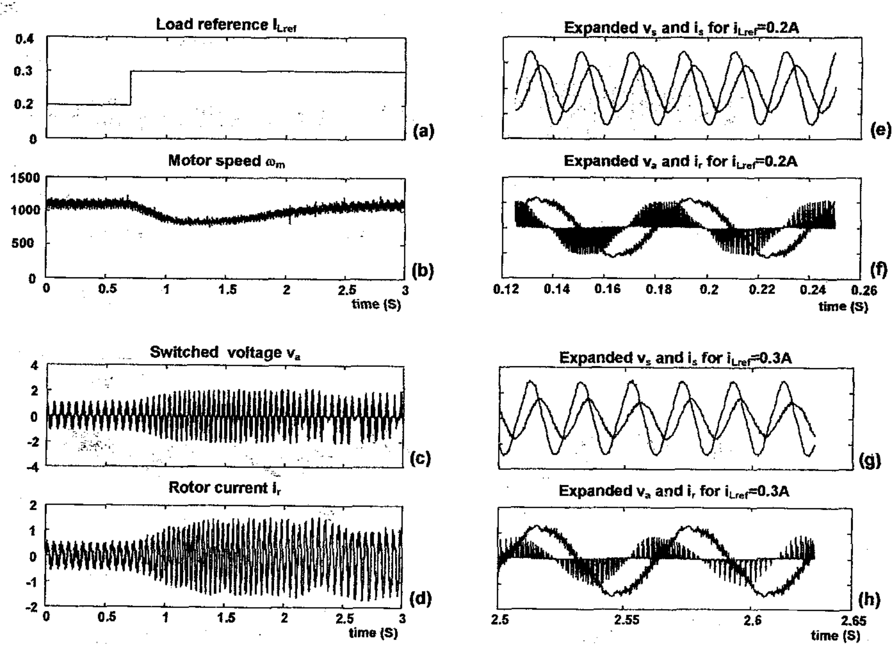

Fig. 9. Experimental results for closed loop motor control with synchronized switching frequency for load variation with constant speed reference at V_s=220V.

7. Conclusions

The present paper deals with the implementation of a synchronized PWM in conjunction with closed-loop control of wound rotor IM. The synchronized modulator has employed a PWM transistor-controlled capacitive network in rotor circuit with a carrier frequency proportional to the rotor voltage frequency. It has been shown that, the modulator maintain the number of switching pulses for the rotor voltage always fixed which exhibit quarter wave symmetry and reduce the sub-harmonic current component, especially at lower switching frequency. The mathematical analysis shows that, the naturally variable phase and magnitude of the switched capacitor voltage has been changed to fixed phase and magnitude for wide range of motor speed. With this property, the effect of the rotor capacitor, which can be optimally chosen at a certain speed and switching frequency to give minimum low order harmonic currents, remains valid for a wide range of motor speed. A power factor improvement is necessarily obtained by this harmonic content reduction. Simulations and experimental results have been shown to be in good agreement with the mathematical analysis.

The proposed modulator is also valid for the PWM inverter feeding the stator of the ac drives recently developed with vector control, direct torque, and space vector techniques. These techniques have the same drawbacks of the system under consideration when using a fixed-frequency switching that affects the drive performance.

References

1] S. R. Bowes, " Advanced regular-sampled PWM control techniques for drives and static power converters", IEEE Trans. on Industrial Electronics, vol. 42, no.4, Aug. 1995. pp 367-373.

2] J. Holtz and B. Beyer, " Optimal synchronous pulse width modulation with a trajectory-tracking scheme for high-dynamic performance", IEEE Trans. on Industry Applications, vol. 29, no. 6, Nov/Dec. 1993. pp1098-1105

3] J. Hamman and L. P. Du Toi, "A New micro-computer controller modulator for PWM inverters", IEEE Trans. on Industrial Applications, vol. IA-22, no. 2, March/April 1986. pp281-285.

4] Y. Iwaji and S. Fukuda, "A pulse frequency modulated PWM inverter for induction motor drives", IEEE Trans. on Power Electronics, vol.7, no. 2. April 1992. pp404-410.

5] J. Richardson, and O. T. Kukrer, "Implementation of a PWM regular sampling strategy for AC drives", IEEE trans. on Power Electronics, vol. 6, no.4, October 1991. pp 645-655.

6] S. R. Bowes, "Novel real-time harmonic minimized PWM control for drives and static power converters", Applied power Electronics Conference and Exposition, APEC' 1993. pp 561-567

7] S. R. Bowes, "Efficient microprocessor real-time PWM drive control using regular-sampled harmonic minimization techniques", IEEE Industrial electronics, ISEI' 93, Budapest, 1993. pp 211-218.

8] J. C. SALMAN, "Selecting stepped reference wave forms for PWM inverter drives to minimize the current distortion", IEEE Industry Applications Society Annual Meeting, vol. 1, 1990. pp 703-710.

9] J. Reinert and G. Parsley, "Controlling the speed of an induction motor by resonating the rotor circuit", IEEE trans. on Industry Applications, vol.31, no. 4, July / August 1995. pp 887-891.

10] M. Ramamooryty, and M. Arunachalam, " Dynamic performance of a closed loop Induction motor speed control system with phase controlled SCR' s in rotor", IEEE Trans. on Industrial Applications, vol. IA-15, no. 5, Sept./Oct. 1979. pp 484-493.

11] S. Lesar, M. S. Smiai, and W. Shephert, "Control of wound rotor induction motor using thyristor in the secondary circuits", IEEE Trans. on Industrial Applications, vol. 32, no. 2, March/April 1996. pp 335-344

12] A. El-Sabbe, M. E. Abdel-Karim, and F. E. Abdel-Kader, "A new thyristor control for wide and stable speed variation of induction motors," MEPCON' 98, Mansoura, Egypt, Dec. 15-17, 1998. pp. 585-592

13] A. E. Lashine, S. M. R. Tahoun, and F. A. saafan, "A new approach to the speed control of wound rotor induction motors", Alexandria Engineering Journal, vol. 38, no. 3, May 1999. pp. B75-B85
14] S. A. Mahmoud, A. E. Lashine, and S. A. Hassan, "Torque / speed control of wound rotor induction motors using a dc chopper circuit", Electric machine and Power System, vol. 11, 1986. pp 25- 38
15] C. S. Moo, C. C. Wei, and C. L. Huang, " Hybrid model for dynamic simulation of solid-state controlled induction machine", Electric Machine and Power Systems, vol. 17, 1989. pp 269-282
16] C. T. Liu, and W. L. Chang, " A generalized technique for modeling switch-controlled induction machine circuits", IEEE Trans. on Energy conversion, vol. 7, no. 1, March 1992. Pp168-176
17] B. C. Kuo, "Digital control systems" Saunders College Publishing, 1992. (Book)

Appendix

- Specification of tested induction motor: V_s=220 V, 2p=4, f=50 Hz, n_m=1340rpm, I_s=1.16A.

Appropriate calculations of no load, locked rotor tests, and open circuit tests gave the following results: r_s=35Ω ℓ_s=0.17H r_r=2.1Ω
ℓ_r=0.0106H r_m=3400Ω ℓ_m=0.99H
Primary / secondary transformation ratio=4
β=0.00075 N-m /rad /sec.
J (motor-load inertia)=0.00035 N. m /rad / sec^2

- Specifications of separately excited dc machine: 220V, 1.2A, 1500rpm and field voltage is 220v.

تقليل التوافقيات الناتجة عن التحكم فى سرعة المحركات التأثيرية ذات العضو الدائري الملفوف باستخدام معدل نبضات تذامنى

د/ مصطفى السيد عبد الكريم
قسم هندسة القوى والآلات الكهربية
كلية الهندسة – جامعة طنطا

ملخص البحث

تعتبر دوائر القدرة الإلكترونية المصدر الرئيسي للتوافقيات فى أنظمة التسيير الكهربي. ويقدم هـذا البحـث دراسة تحليلية و معملية لطريقة جديدة لتقليل التوافقيات لمحرك تأثيري يتم التحكم فى سرعته عن طريق مجموعة مكثفات متصلة بعضوه الدوار باستخدام حاكم تناسبي– تكاملي. وتعتمد طريقة التحكم هذه على اسـتخدام مكثفات متساوية السعة متصلة نجمة فى دائرة العضو الدوار يتم التحكم فيها عن طريق أربعة مفاتيح إلكترونيـة سريعة يمكنها تمرير التيار فى كلا الاتجاهين باستخدام قنطرة من أربعة موحدات سريعة لكل مفتـاح. ويمكـن التحكم بنعومة فى السرعة بالتحكم فى فترة اتصال المكثفات بدائرة العضو الدوار بالنسبة لفـترة اسـتبعادها وقصر دائرة العضو الدوار وبالتالي يمكن التحكم فى جهد المكثفات والذي يعمل كمصدر جهد ثلاثي الأوجـه مضاد لجهد العضو الدوار وله نفس تردده ويتم إدخال المكثفات أو إبعادها فى دائرة العضو الدوار بأسـلوب التعديل النبضي لموجة جهد المكثفات.

وقد أثبتت الدراسة انه عند استخدام تردد ثابت لمعدل النبضات أن قيمة وزاوية جهد المكثفات المقطع علـى دائرة العضو الدوار تتغيران مع تغير تردد جهد العضو الدوار ليسبب بدورة توافقيـات متغـيرة فى تيـارات المحرك. وفى هذا البحث تم اقتراح طريقة لتغيير تردد معدل النبضات ليكون متزامنا مع تردد جـهد العضـو الدوار بحيث تحتفظ دورة جهد المكثفات المقطع على دائرة العضو الدوار دائما بعدد ثابت من النبضات مـع تغيير سرعة المحرك. أثبتت الدراسة النظرية للطريقة المقترحة أن معدل النبضات المتزامن يعمل على تثبيت قيمة وزاوية جهد المكثفات المقطع عند تغيير سرعة المحرك. وبوجود هذه الخاصية يمكن الحفاظ – لمدى واسع مـن السرعات– على اقل قيمة لتوافقيات تيار المحرك تم الحصول عليها مسبقا عند قيمة معينة لكل من سعة المكثـف وتردد التقطيع وسرعة المحرك.

تم تحليل النظام وبناء النموذج النظري حيث ظهر توافقا جيدا بين النتائج النظرية والمعملية وأوضحت كل مـن النتائج المعملية والمحسوبة نظريا أن استخدام هذه الطريقة يؤدى إلى تقليل التوافقيات فى تيار المحرك وتحسـين معامل القدرة مقارنتا باستخدام معدل نبضات ذو تردد ثابت.